Demodulation Methods for a Wireless Electromagnetic Tracker

François Guerret, Pauline Vehrlé, Hendrik Meier, Antoine Girard, Christophe Prieur

Demodulation Methods for a Wireless Electromagnetic Tracker

François Guerret[1,2], Pauline Vehrlé[1], Hendrik Meier[1], Antoine Girard[2] and Christophe Prieur[3]
[1]Sysnav, 27200 Vernon, France
[2]Université Paris-Saclay, CNRS, CentraleSupélec, Laboratoire des signaux et systèmes, 91190 Gif-sur-Yvette, France
[3]CNRS, Univ. Grenoble Alpes, Grenoble-INP, GIPSA-lab, F-38000 Grenoble, France

Abstract—To tackle the demodulation issues of wireless electromagnetic trackers, we propose a method that takes advantage of non-orthogonalities between the coils of the emitter. This method does not require an additional sensor, nor a synchronization signal, nor an initialization step. It can therefore be combined with a tracking method to make it robust to a loss of signal.

I. INTRODUCTION

Electromagnetic trackers (EMT) are popular [1] positioning systems, without the need for a line of sight, that use magnetic fields to estimate the pose (position and orientation) of a sensor (receiving antennae) with respect to a transmitter, whose antennae generate the magnetic fields. The generated fields can be either pulsed constant fields (e.g. [2]) or alternating fields (e.g. [3], [4]). In either case, they are usually produced by orthogonal coils that mainly behave as magnetic dipoles. To identify, on the *sensor* side, the contribution of each coil of the *transmitter*, systems generating constant fields use time multiplexing – each coil is powered alternately in predefined slots of time – whereas systems generating alternating fields use frequency multiplexing – each coil is powered at a different frequency. This identification step is called "demodulation" for alternating fields.

The company *Sysnav* developed an EMT using alternating magnetic fields and, by developing ideas close to the ones presented in [5] and [6], improved the dipole model of fields usually used to extract poses from field measurements in order to reach higher performances.

Wireless EMT have been developed [7]–[11] to increase the field of application of trackers. Their main advantage is the freedom of movement they offer. Different strategies have been implemented to provide this feature. For instance, the *sensors* of the apparatus studied in [10] are actually transponders: no measurement is performed on the *sensor* side but the field generated by the *sensor* coil to be localized – which is the consequence of the induced current in the coil – is itself measured by other *sensors*. A similar strategy is described in another context in [12]. Another method is the one used by *Google* [7], *Polhemus* [8], [9] or Yang and al. [11]: the *transmitter* is wired to a board in charge of powering its coils and the *sensor* is wired to another board in charge of measuring the induced current in the *sensor* coils and of performing the demodulation. After demodulation, data is sub-sampled and, depending on the application, the extraction of the pose can be done in the *sensor* board or in a separated processing unit. This second strategy has been followed to develop a wireless system from the *Sysnav* EMT such that no physical link remains between the *transmitter* and the *sensor*.

After having presented the principles of the method to extract a pose from magnetic fields measurements, we focus in this paper on the different variants of asynchronous demodulation that can be performed. We introduce in particular a demodulation method that does not require an external device bounded to the *sensor* nor an initialization step. Finally, we briefly present some validation results of this method which has been tested on simulation data and on real data, retrieved from a wireless EMT prototype.

II. EXTRACTING POSES FROM MAGNETIC FIELDS

A. Constant Magnetic Fields

The magnetic field produced by an ideal coil powered with a constant signal can be approximated by a magnetic dipole of moment $\boldsymbol{m}$ far from the coil. For a coil centered at the origin of the frame and which axis is directed by $\boldsymbol{e}_z$, the moment of the dipole can be written $m\boldsymbol{e}_z$ and the generated field at a position $\boldsymbol{r} = (x, y, z)^T$ is, in Cartesian coordinates:

$$\boldsymbol{b}_z(\boldsymbol{r}) = \frac{\mu_0 m}{4\pi r^5}(3xz, 3yz, 3z^2 - r^2)^T \tag{1}$$

where r denotes the norm of $\boldsymbol{r}$ and μ_0 is the vacuum permeability.

Assuming that the three *transmitter* coils are perfectly identical and are oriented such that their directions form a direct frame, these emitted fields measured at a given pose can be gathered in a matrix, that is given by:

$$\boldsymbol{M'} = \frac{\mu_0 m}{4\pi r^5}(3\boldsymbol{r}\boldsymbol{r}^T - r^2\boldsymbol{I_3}) \tag{2}$$

Each column of $\boldsymbol{M'}$ describes the field generated by one coil of the *transmitter*, measured at $\boldsymbol{r}$. Considering that the *sensor*, whose orientation relative to the *transmitter* frame is denoted as $\boldsymbol{R} \in \mathrm{SO}_3(\mathbb{R})$, can measure the field along three orthogonal directions, the measurements along each axis are described by a line of the "magnetic matrix" defined as: $\boldsymbol{M} = \boldsymbol{R}^T\boldsymbol{M'}$.

To extract a pose from a magnetic matrix built from measurements, the following algorithm, detailed in [13], can be applied:

1) Compute a Singular Value Decomposition (SVD) of $\boldsymbol{M} = \boldsymbol{P}\boldsymbol{S}\boldsymbol{Q}^T$ such that $\boldsymbol{S}$ is a diagonal matrix of positive real values ordered such that $S_{11} \geq S_{22} \geq S_{33}$.
2) The distance to origin can be computed as: $r = \left(\frac{4\mu_0 m}{4\pi Tr(\boldsymbol{S})}\right)^{1/3}$
3) The orientation of the *sensor* can be retrieved with $\boldsymbol{R} = \boldsymbol{Q} \cdot \mathrm{diag}\,(1, -1, -1) \cdot \boldsymbol{P}^T$
4) And the position of the *sensor* is given by the first column of $\boldsymbol{Q}$: $\boldsymbol{r} = \pm r(Q_{11}, Q_{21}, Q_{31})^T$.

A simple criterion permits to detect whether a matrix belongs to the set of possible magnetic matrices or not. Such metric can be used as a criterion to be minimized to perform optimizations in charge of identifying parameters of models for instance. From the algorithm presented above, we propose to build the criterion:

$$C_M : \boldsymbol{M} = \boldsymbol{P}\boldsymbol{S}\boldsymbol{Q}^T \mapsto \left(\frac{(S_{11} - 2S_{22})^2 + (S_{11} - 2S_{33})^2}{S_{11}^2 + 4S_{22}^2 + 4S_{33}^2}\right)^{\frac{1}{2}} \tag{3}$$

This criterion satisfies the following property:

$$\begin{aligned}\forall A \in \mathrm{GL}_3(\mathbb{R}) : C_M(\boldsymbol{A}) = 0 \text{ and } \det(\boldsymbol{A}) > 0 \iff \\ \exists \boldsymbol{R} \in \mathrm{SO}_3(\mathbb{R}), \exists \boldsymbol{u} \in \mathbb{S}^2, \boldsymbol{A} \propto \boldsymbol{R}^T\left(3\boldsymbol{u}\boldsymbol{u}^T - \boldsymbol{I}_3\right)\end{aligned} \tag{4}$$

B. Alternating Magnetic Fields: Demodulation

When AC magnetic fields are used, the magnetic matrix $\boldsymbol{M}$ must be obtained by demodulation so that the *sensor* pose can be retrieved as above.

Each coil of the *transmitter* generates the field of a magnetic dipole $m_j(t)\boldsymbol{e}_j$ where the constant unitary vector $\boldsymbol{e}_j$ directs the coil and where $m_j(t)$ oscillates at the angular frequency ω_j (with $\omega_k \neq \omega_j$ if $k \neq j$). The induced voltage in a *sensor* coil i can be written:

$$u_i(t) = -\sum_{j=1}^{3} N_i \int_{S_i} \dot{\boldsymbol{b}}_j(t) \cdot \boldsymbol{n_i} \mathrm{d}^2 S = \sum_{j=1}^{3} u_{ij}(t) \tag{5}$$

where N_i is the number of loops of the coil i, $\boldsymbol{b_j}$ is the field produced by the coil j of the *transmitter*, $\boldsymbol{n_i}$ is the normalized vector orienting all the loops of a given *sensor* coil and S_i is the surface of each loop of this coil. Thus, u_{ij} denotes the part of the potential difference measured in the *sensor* coil i due to the field emitted by the *transmitter* coil j (at its specific frequency).

The demodulation is straightforward if the current powering the *transmitter* coils $i_j(t)$ and the potential measured in the *sensor* $u_i(t)$ can be measured synchronously (at the same instant or such that the relative date of sampling can be reconstituted). For instance, if we assume that $i_j(t) = I_j \cos(\omega_j t)$ (where I_j denotes the semi-amplitude of $i_j(t)$), the "signed" semi-amplitude U_{ij} of u_{ij} (positive if u_{ij} is in phase with i_j, negative otherwise) can be retrieved with:

$$U_{ij} = \frac{2\mathcal{F}_{lp}\left[u_i(t - \frac{\pi}{2\omega_j}) \times i_j(t)\right]}{I_j} \tag{6}$$

where $\mathcal{F}_{lp}[\bullet]$ denotes a low-pass filtering. The time shift in u_i is necessary to compensate the phase shift of $\frac{\pi}{2}$ due to the magnetic induction. The low-pass filter and the frequencies must be chosen such that for all k, j, $|\omega_k - \omega_j|$ is larger than the band pass of $\mathcal{F}_{lp}$, so that $\cos((\omega_k - \omega_j)t)$ is efficiently cut.

In a wireless EMT, because two different boards are now in use, an issue arises due to the relative drift between the clock driving the current in *transmitter* coils and the one performing the sampling on *sensor* side. In general, clocks providing the base time on the boards drift slowly and randomly (depending of environment variations) with respect to each other. A typical upper bound for these relative drift is 40 µs per second (example of crystals clocking at 33 kHz ± 20 ppm).

On such systems, the demodulation can be performed by multiplying $u_i(t)$ by a cosine and/or a sine signal generated at the rhythm of the *sensor* board clock. The main idea of *synchronous* demodulation is to generate such "demodulation signals" (a.k.a "reference signals" [14]) with the appropriate frequency and phase, such that the *transmitter* signals and the demodulation signal remain in phase. To do so, a synchronization signal can be sent from the *transmitter* board. This can be done with a dedicated transmitter or by periodically sending a beacon in the signals in the *transmitter* coils. In practice, these methods are quite heavy to implement (corrections array must be embedded to generate a corrected demodulation signal) and either require additional components to be added to the system or reduce the availability of the measurements.

III. ASYNCHRONOUS DEMODULATION

A. General Principles

In general, the measured induced voltage u_i can be written as:

$$u_i(t) = \sum_{j=1}^{3} U_{ij} \cos(\omega_j t + \varphi_{ij}(t)) \tag{7}$$

where $\varphi_{ij}(t)$ is due to relative clock drift and varies slowly. To identify the phase $\varphi_{ij}(t)$ modulo π, it is enough to use two demodulation signals $\cos(\omega_j t)$ and $\sin(\omega_j t)$:

$$\varphi_{ij}(t) = \arctan\left(\frac{\mathcal{F}_{lp}\left[u_i(t) \times \sin(\omega_j t)\right]}{\mathcal{F}_{lp}\left[u_i(t) \times \cos(\omega_j t)\right]}\right) \mod \pi \tag{8}$$

The results of the proposed demodulation filtering gives also immediately the norm of U_{ij}:

$$|U_{ij}| = 2\left(\mathcal{F}_{lp}\left[u_i(t) \times \sin(\omega_j t)\right]^2 + \mathcal{F}_{lp}\left[u_i(t) \times \cos(\omega_j t)\right]^2\right)^{1/2} \tag{9}$$

An asynchronous demodulation based on this principle is proposed in [14]. However, to determine the signs of U_{ij} (i.e. to determine the value of $\varphi_{ij}(t)$ modulo 2π), [14] requires a common generator of demodulation signal on *transmitter* side and on *sensor* side – and gathering non-demodulated data on the same board has an important cost in data transmission bandwidth or requires a lower sampling frequency that implies loosing precision.

We can assume without loss of generality that for all i and for all j, $\varphi_{ij} = \varphi_j$, that is to say that the phase due to clock drifts only depends on the frequency and not on the *sensor* coil (in practice a constant phase gap between the acquisition tracks may exist but its calibration and correction is not difficult). This point is important for the robustness of the algorithm because it states that we can compute φ_j from (8) with the index i that maximises the signal to noise ratio of u_{ij}, i.e. with $i = \underset{i \in \{1,2,3\}}{\operatorname{argmax}}\left(|U_{ij}|\right)$.

We can now build a matrix $\boldsymbol{M^m}$ such that $\boldsymbol{M^m_{ij}} = \operatorname{Sign}\left(\mathcal{F}_{lp}\left[u_i \times \sin(\omega_j t)\right]\right)|U_{ij}|$ or $\boldsymbol{M^m_{ij}} = \operatorname{Sign}\left(\mathcal{F}_{lp}\left[u_i \times \cos(\omega_j t)\right]\right)|U_{ij}|$, the first equality being used if $|\mathcal{F}_{lp}\left[u_i \times \sin(\omega_j t)\right]| > |\mathcal{F}_{lp}\left[u_i \times \cos(\omega_j t)\right]|$. Thus, if the magnetic fields are perfectly dipolar, $\boldsymbol{M^m}$ matches the theoretical magnetic matrix, except for its signs which are only known relatively to each other inside each column j. Given that $\det(\boldsymbol{M}) > 0$, the true magnetic matrix satisfies:

$$\begin{gathered}\boldsymbol{M} \in \{\boldsymbol{M^m \Xi} \mid \boldsymbol{\Xi} \in \mathcal{S}_\Xi\}, \text{ with:} \\ \mathcal{S}_\Xi = \{\boldsymbol{I_3}, \operatorname{diag}(-1,-1,1), \operatorname{diag}(-1,1,-1), \operatorname{diag}(1,-1,-1)\}\end{gathered} \tag{10}$$

We denote $\boldsymbol{\Xi^*}$ the matrix such that $\boldsymbol{M} = \boldsymbol{M^m \Xi^*}$. The main issue is that for a given pose $(\boldsymbol{r}, \boldsymbol{R})$, we can write:

$$\begin{gathered}\forall \xi \in \{-1,1\}, \forall \boldsymbol{\Xi} \in \mathcal{S}_\Xi, \\ \boldsymbol{M\Xi} = \frac{\mu_0 m}{4\pi r^5}(\boldsymbol{\Xi R})^T\left(3(\xi \boldsymbol{\Xi r})(\xi \boldsymbol{\Xi r})^T - r^2 \boldsymbol{I_3}\right)\end{gathered} \tag{11}$$

Thus, we cannot identify the magnetic matrix $\boldsymbol{M}$ among the 4 candidates of (10) by self-consistency of the system because for any $\boldsymbol{\Xi}$ in $\mathcal{S}_\Xi$, $\boldsymbol{M\Xi}$ is a perfectly valid magnetic matrix (it is the magnetic matrix of the poses $(\xi \boldsymbol{\Xi r}, \boldsymbol{\Xi R})$).

The unknown ξ is due to the central symmetry of the problem and is proper to any tri-axis EMT system. To determine the half-space, an external sensor that provides an approximate pose can be used (as in [7]) or a tracking of the current half-space from a known initial

half-space (as in [15]) can be performed. These solutions can be adapted to identify $\boldsymbol{\Xi}$, as explained in the next subsection.

B. Tracking Solutions

Pose tracking consists in performing an initialization (the *sensor* must be brought to a known pose), then maintaining the current pose of each sample by choosing the candidate whose pose is the closest to the pose estimated at the previous sample.

Phase tracking consists in identifying the quadrant of $\varphi_j(t)$ knowing the phase value modulo π and the phase at date $t-\tau$ modulo 2π: it is enough to choose φ_j such that $|\varphi_j(t)-\varphi_j(t-\tau)| < \frac{\pi}{2}$. The updating period τ being chosen so that $\tau\dot{\varphi} < \frac{\pi}{2}$. The initialization is performed by comparing the signs of $\boldsymbol{M}^m$ to the expected magnetic matrix at a pose where the sensor is known to be approximately placed.

The tracking methods (used for instance in [16]) have two main drawbacks: they require an initialization step and they are sensible to a loss of signal, which may occur if the *sensor* is moved out of reach of the *transmitter* signals or if a strong disturber masks the signals from the *transmitter* for a while. Another solution that does not require such initialization can be proposed: it consists in breaking artificially the symmetry of the problem by adding defects to the system of *transmitter* coils.

C. Taking Advantage of Non-Orthogonalities of the Coils

Various modification of the shape of the *transmitter* can be used to break symmetries of the problem and identify ξ and $\boldsymbol{\Xi}$ that lead to the real pose among the candidates. We focused on the choice of $\boldsymbol{\Xi}$ and chose to introduce asymmetries with a long-range impact: we studied how to take advantage of non-orthogonalities between the coils of the *transmitter*.

Non-orthogonalities of the *transmitter* coils can be modelled by an upper triangular matrix $\boldsymbol{B}$ such that $\boldsymbol{M}_{\text{measured}} = \boldsymbol{M}_{\text{theoretical}}\boldsymbol{B}$. It is physically described by: $\boldsymbol{B} = \begin{pmatrix} 1 & -\sin(\theta) & \sin(\phi)\cos(\psi) \\ 0 & \cos(\theta) & \sin(\phi)\sin(\psi) \\ 0 & 0 & \cos(\phi) \end{pmatrix}$, where the angles between coils are specified on Fig. 1a. This is a direct consequence of the linearity of the dependency of the magnetic fields to the dipole moments of the *transmitter*. The coefficients of $\boldsymbol{B}^{-1}$ can be identified in calibration by minimizing the mean $C_M(\boldsymbol{M}_{\text{measured}}\boldsymbol{B}^{-1})$ over a set of points well distributed around the *transmitter*. The main idea is

Table 1: Approximate Poses $\boldsymbol{u} \in \mathbb{S}^2$ for Which $C_M(\boldsymbol{M}(r\boldsymbol{u})\boldsymbol{\Xi}\boldsymbol{B}^{-1}) = 0$

$\boldsymbol{\Xi}$	$\boldsymbol{u}$ for which $C_M(\boldsymbol{M}(r\boldsymbol{u})\boldsymbol{\Xi}\boldsymbol{B}^{-1}) = 0$
diag $(-1,-1,1)$	$\pm\begin{pmatrix}0\\0\\1\end{pmatrix}, \frac{\pm1}{\sqrt{B_{13}^2+B_{23}^2}}\begin{pmatrix}B_{13}\\B_{23}\\0\end{pmatrix}$
diag $(-1,1,-1)$	$\pm\begin{pmatrix}0\\1\\0\end{pmatrix}, \frac{\pm1}{\sqrt{B_{12}^2+B_{23}^2}}\begin{pmatrix}B_{12}\\0\\B_{23}\end{pmatrix}$
diag $(1,-1,-1)$	$\pm\begin{pmatrix}1\\0\\0\end{pmatrix}, \frac{\pm1}{\sqrt{B_{12}^2+B_{13}^2}}\begin{pmatrix}0\\B_{12}\\B_{13}\end{pmatrix}$

to identify the best candidate among (10) with:

$$\boldsymbol{\Xi}^* = \underset{\boldsymbol{\Xi}\in\mathcal{S}_{\boldsymbol{\Xi}}}{\operatorname{argmin}} \left(C_M\left(\boldsymbol{M}^m\boldsymbol{\Xi}\boldsymbol{B}^{-1}\right)\right) \tag{12}$$

We can show (the proof is omitted here because of space constraints) that for any $\boldsymbol{\Xi} \neq \boldsymbol{\Xi}^*$, $C_M(\boldsymbol{M}^m\boldsymbol{\Xi}\boldsymbol{B}^{-1}) > 0$ is verified almost everywhere. $C_M(\boldsymbol{M}^m\boldsymbol{\Xi}\boldsymbol{B}^{-1})$ is null if and only if the position of the *sensor* belongs to one of 4 rays (per $\boldsymbol{\Xi}$) at most, i.e. if and only if $\boldsymbol{r}$ is proportional to one of 4 positions on the unit sphere. These positions on $\mathbb{S}^2$ can be approximated; they are listed in Table 1. Thus, in free space, (12) can be theoretically used to identify the $\boldsymbol{M} = \boldsymbol{M}^m\boldsymbol{\Xi}^*\boldsymbol{B}^{-1}$ almost everywhere.

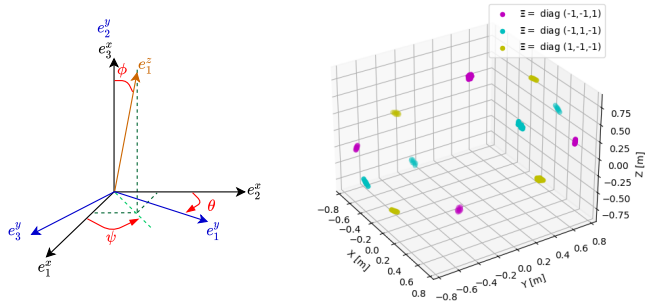

(a) (b)

Fig. 1: (a) Angles between the coils. e_1^* is the vector directing the coil $*$ ($*$ denotes the main axis of the coil) and $e_{2,3}^*$ are chosen such that $(e_i^*)_i$ form a direct orthonormal basis. (b) Positions around the unit sphere at which (12) cannot be used since one invalid $\boldsymbol{\Xi}$ leads to a C_M close to 0 (arbitrary threshold chosen).

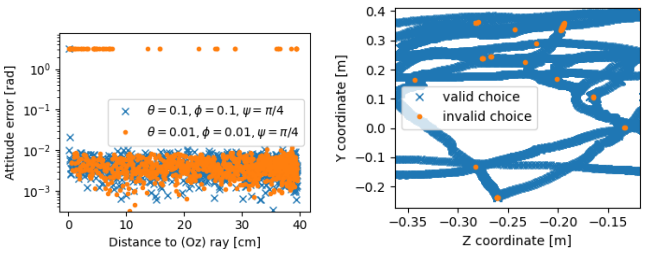

(a) (b)

Fig. 2: (a) Error in attitude along a simulated trajectory on the unit sphere after pose extraction on a strongly noised signal and variable φ_{ij} ($\dot{\varphi}_{ij} \approx 1\,\text{rad}\,\text{s}^{-1}$) for two different sets of non-orthogonalities. A wrong choice of $\boldsymbol{\Xi}$ leads to an error in attitude close to π rad. (b) Experimentally measured trajectory of a wireless *sensor* obtained by performing a phase-tracking demodulation (reference) and, independently, a demodulation using the identification of $\boldsymbol{\Xi}^*$ with (12). The choice of $\boldsymbol{\Xi}^*$ is valid almost everywhere.

IV. VALIDATION

A simulator has been developed to generate data that could be measured in a *sensor* along any trajectory. It has been used to test the demodulation algorithms, the correction of defects, the pose extraction algorithm, and the theoretical results on the use of non-orthogonalities between the coils of the *transmitter* to find $\boldsymbol{\Xi}^*$, in particular to confirm that the set of areas in which (12) cannot be used is reduced to 12 rays, as illustrated on Fig. 1b. In practice, even after corrections, the measured magnetic matrix does not perfectly match the theoretical one (for instance when magnetic noise around the working frequencies is present), so (12) may give a wrong result in extended spaces around the rays. To reduce the size of these

spaces, the angles defining the non-orthogonalities can be increased. The impact of the choice of these angles in the context of a strongly noised signal (produced by simulation) is illustrated on Fig. 2a.

The phase-tracking solution has been tested on real data acquired from a wireless EMT prototype. The performances reached are similar to the one reached with the *Sysnav* EMT prototype in which the *transmitter* is driven by the board that also samples *sensor* data. Concerning the use of asymmetries, originally unintended defects of the tested *transmitter* prototype have been proved sufficient to identify the right candidate matrix in the main part of trajectories acquired by performing smooth random movements in free space. An example of trajectory is presented in Fig. 2b: it shows a space in which the choice made in (12) leads almost everywhere to the same matrix $\boldsymbol{M} = \boldsymbol{M}^m \boldsymbol{\Xi}^* \boldsymbol{B}^{-1}$ as the one retrieved thanks to the tracking method. The covered area has been chosen close enough to the *transmitter* (where the signal-to-noise ratio of the EMT is sufficient) and not too close to the theoretically uncertain spaces depicted in Fig. 1b. The few points where the identification failed are probably due to too fast changes of orientation and can be filtered out.

Finally, to improve the robustness of the system, the two methods can be combined: the (re-)initialization step required for tracking can be provided by an identification of $\boldsymbol{\Xi}^*$ with (12) by simply moving the *sensor* into an area where the choice is not ambiguous, for instance anywhere into the area covered by the trajectory plotted on Fig. 2b.

V. CONCLUSION

Several approaches to tackle the demodulation issues of wireless electromagnetic trackers have been described in this paper, in particular a self-consistent demodulation method that takes advantage of non-orthogonalities between the coils of the *transmitter*. This method, which does not require an additional sensor, nor a synchronization signal, nor an initialization step, has been proved to be reliable on real data in free space and on simulation data in the presence of disturbers (with bigger non-orthogonality angles than the ones of the tested *transmitter* prototypes).

The use of a *transmitter* with willingly added non-orthogonalities (dimensioned after optimizations on simulated data) to improve the robustness to noise is presently under test. It is also the case of a method that combines the use of asymmetries with the phase-tracking algorithm.

REFERENCES

[1] E. Prigge and J. How, "An indoor absolute positioning system with no line of sight restrictions and building-wide coverage," *Virtual Reality*, 2000.

[2] P. T. Anderson, "Pulsed-DC position and orientation measurement system," U.S. Patent 5,453,686, 1993.

[3] F. H. Raab, E. B. Blood, T. O. Steiner, and H. R. Jones, "Magnetic position and orientation tracking system," *IEEE Transactions on Aerospace and Electronic Systems*, vol. AES-15, no. 5, pp. 709–718, 1979.

[4] C. Constant, "Mesure de l'orientation relative de deux corps et système de repérage de direction correspondant," France Patent 79 14 441, 1979.

[5] J. Lescourret, "Method for determining the position and the orientation of a movable object, especially the line-of-sight of a helmet-mounted visor." France Patent FR 2,734,900 / EP 0,745,827, 1995.

[6] H. R. Jones Jr., "Non-concentricity compensation in position and orientation measurement system," U.S. Patent 5,307,072, 1992.

[7] S. Chung, I. Atkinson, A. Jain, L. Organesian, M. Stein, and S. Patkar, "Correcting field distortion in electromagnetic position tracking systems," U.S. Patent 10 746 819B2, 2020.

[8] Polhemus, "Patriot wireless," Colchester, Vermont, US, 2008. [Online]. Available: https://polhemus.com/motion-tracking/all-trackers/patriot-wireless

[9] ——, "G4," Colchester, Vermont, US, 2010. [Online]. Available: https://polhemus.com/motion-tracking/all-trackers/g4

[10] C. Silva, D. Mateus, M. Eiras, and S. Vieira, "Calypso 4D localization system: a review," *Journal of Radiotherapy in Practice*, vol. 13, no. 4, p. 473–483, 2014.

[11] W. Yang, C. Zhang, H. Dai, C. Hu, and X. Xia, "A novel wireless 5-D electromagnetic tracking system based on nine-channel sinusoidal signals," *IEEE/ASME Transactions on Mechatronics*, vol. 26, no. 1, pp. 246–254, 2021.

[12] I. Khalfin and H. S. Jones Jr., "Electromagnetic position and orientation tracking system with distortion compensation employing wireless sensors," U.S. Patent 6,369,564, 2002.

[13] H. Meier, M. Hillion, and D. Vissière, "Method for locating an object moving in a magnetic field generated by an assembly of at least three magnetic generators," France Patent FR 3 069 068 / CA 3 069 366, 2018.

[14] K. O'Donoghue and P. Cantillon-Murphy, "Low cost super-nyquist asynchronous demodulation for use in em tracking systems," *IEEE Transactions on Instrumentation and Measurement*, vol. 64, no. 2, pp. 458–466, 2015.

[15] H. Wu, Y. Zhao, and C. Zhang, "Efficient hemisphere unambiguous magnetic positioning for helmet mounted sights," in *2018 IEEE/AIAA 37th Digital Avionics Systems Conference (DASC)*, 2018, pp. 1–6.

[16] R. F. Higgins, H. R. Jones Jr., and A. G. Rodgers, "AC magnetic tracking system with non-coherency between sources and sensors," U.S. Patent 2008/0 120 061 A1, 2008.